# The Effect of Fiber Concentration on Mechanical and Thermal Properties of Fiber-Reinforced Polypropylene Composites

**S. Houshyar, R. A. Shanks, A. Hodzic**

*Applied Chemistry, RMIT University, GPO Box 2476V, Melbourne, 3001, Australia*

Received November 11, 2003; accepted 26 April 2004
DOI 10.1002/app.20874
Published online in Wiley InterScience (www.interscience.wiley.com).

**ABSTRACT:** A novel composite material consisting of polypropylene (PP) fibers in a random poly(propylene-*co*-ethylene) (PPE) matrix was prepared and its properties were evaluated. The thermal and mechanical properties of PP–PPE composites were studied by dynamic mechanical analysis (DMA) and differential scanning calorimetry (DSC) with reference to the fiber concentration. Although, by increasing PP fiber concentration in PPE, no significant difference was found in melting and crystallization temperatures of the PPE, the storage, and the tensile and flexural modulus of the composites increased linearly with fiber concentrations up to 50%, 1.5, 1.0, 1.3 GPa, respectively, which was approximately four times higher than that for the pure PPE. There is a shift in glass transition temperature of the composite with increasing fiber concentration in the composite and the damping peak became flatter, which indicates the effectiveness of fiber–matrix interaction. A higher concentration of long fibers (>50% w/w) resulted in fiber packing problems, difficulty in dispersion, and an increase in void content, which led to a reduction in modulus. Cox–Krenchel and Haplin–Tsai equations were used to predict tensile modulus of random fiber-reinforced composites. A Cole–Cole analysis was performed to understand the phase behavior of the composites. A master curve was constructed based on time–temperature superposition (TTS) by using data over the temperature range from −50 to 90°C, which allowed for the prediction of very long and short time behavior of the composite. © 2005 Wiley Periodicals, Inc. J Appl Polym Sci 96: 2260–2272, 2005

**Key words:** composites; reinforcement; mechanical properties; polypropylene; dynamic mechanical properties

## INTRODUCTION

Fibers are frequently used for improving the strength and rigidity of polymers. Several studies were reported concerning the reinforcement of polypropylene (PP) and other thermoplastic polymers using different types of fibers to achieve improvement in the thermal, structural, and mechanical properties. Among the various fibers, which have been used for composites of PP, glass fibers are the most common. Some fibers induce a transcrystalline morphology as was recently reported to occur in PP when melt crystallized in contact with carbon and aramid fibers. Other polymeric materials including poly(ether ether ketone), nylon-6,6, nylon-6, poly(ethylene terephthalate) (PET), and PP can be crystallized with these fibers.[1,2,3] Apart from the morphological studies, the importance of a transcrystalline interface on the mechanical properties of some fiber-reinforced polymer systems was investigated. In the case of composites, formation of a transcrystalline morphology provided higher interfacial bond strength and a high transverse tensile strength. Therefore, a self-reinforced composite will be expected to show a strong interfacial bonding between the two phases.[4,5] For composites based on semicrystalline polymers, their crystallinity is an important factor, which determines the stiffness of the crystallized matrix. It is known that a transcrystalline layer (TCL) forms at the fiber–matrix interface when fibers with high nucleating ability are employed. Several researchers demonstrated that the TCL of PP and polyethylene (PE) has a less ductile nature and a higher Young's modulus compared with the spherulites in the bulk.[6,7]

The idea of embedding fibers in the same matrix is not new, but, in the case of PP fibers and a PP matrix, it provides some specific features, such as recyclability, ease of production, low cost, and good interfacial bonding without any surface treatment.[8] In addition to these advantages, composites with the same polymer possess good mechanical properties and minimize shear stresses. A literature survey revealed only a few articles that discuss PP composites, which are so-called " all-PP," that are the subject of the present study. These articles are devoted mostly to investigation of transcrystallization growth of PP on the fiber

*Correspondence to:* R. A. Shanks (Robert.shank@rmit.edu.au).
Contract grant sponsor: International Postgraduate Scholarship.


© 2005 Wiley Periodicals, Inc.

surface, preparation, and some mechanical performance of the composite modulus.[9,10,11] In view of the lack of research on PP fibers in a poly(propylene-*co*-ethylene) (PPE) matrix composites, their properties, and the influence of fiber concentration on the properties, this study was undertaken to prepare and investigate the effect of various fiber concentrations on the properties of these composites. In addition, the question of appropriate bonding of the fiber–matrix interface is essential to the formation of effective PP composites. A key to solving this problem is the chemical similarity of the fiber and the matrix.[12,13]

The different structural state of the composite constituents led to an appreciable difference in their melting temperatures (the melting temperatures are 147 and 165°C for PPE matrix and PP fiber, respectively), which provides a sufficiently wide manufacturing temperature window. This window coupled with typical sheath-core morphology of the PP fibers may allow some surface melting of the fiber, without affecting the highly oriented core, thus retaining good mechanical performance. In this case, the outer layer of the fiber could potentially cocrystallize with the matrix at the interface, which can improve bonding between two phases. This anticipation is supported by previous data.[14,15] This may also be a way of obtaining molecular composites, with zones of oriented and unoriented crystallites with no clearly expressed interface.[16,17,18]

The most commonly used theory used to model the stiffness of this type of composite was developed by Cox and further improved by Krenchel. The theory was reviewed by a number of authors.[18,19,20]

A simple rule of mixture approach to the stiffness of a unidirectional continuous fiber-reinforced composite gives the equation

$$E_c = V_f E_f + V_m E_m \tag{1}$$

where $E$ is a tensile modulus, $V$ is a volume fraction, and the subscripts $c$, $f$, and $m$ represent composite, fiber, and matrix, respectively. For a unidirectional composite, a correction factor must be introduced to account for the lengths of fiber not fully contributing to the stiffness of the composite because of the shear stress transfer between each fiber and the matrix. This term $\eta_1$ is defined as

$$\eta_1 = [1 - (\tanh(\beta L/2)/\beta L/2) \tag{2}$$

and the term $\beta$ is given

$$\beta = 2/D[2G_m/(E_f \operatorname{Ln}(r/R)^{0.5}] \tag{3}$$

where $L$ is the fiber length, $G_m$ is the shear modulus of the matrix, $r$ is the fiber radius, and $R$ is related to the mean spacing of the fibers.[1,19]

Consequently, the stiffness of the unidirectional fiber-reinforced composites can be expressed by

$$E_c = \eta_1 V_f E_f + V_m E_m \tag{4}$$

Also, Krenchel extended this theory to take fiber orientation into account by adding a fiber orientation factor $\eta_0$ into the rule of mixture equation giving

$$E_c = \eta_1 \eta_0 V_f E_f + V_m E_m \tag{5}$$

For the random fiber-reinforced composite orientation factor is about 0.375 (3/8) also, and $\eta_1$ is about 1 for continuous or long fiber-reinforced composite[1,19]

$$E_c = 0.375(1 - V_m)E_f + V_m E_m \tag{6}$$

Our earlier studies have proved PP fibers to be an effective reinforcement in PPE matrix. Static and dynamic mechanical test methods were widely employed for investigating the structural, mechanical, and viscoelastic behavior of polymeric materials for determining their relevant stiffness and damping characteristics for various applications.[15] In the present article, we report on the influence of PP fiber on the mechanical and thermal properties of PPE polymer. The effect of fiber concentration, frequency, and temperature on the thermal, structural, and mechanical properties is reported and compared with theoretical prediction. The evaluation of glass-transition temperature ($T_g$) is taken as a measurement of the interfacial interaction and reported as a function of fiber concentration, to characterize the fiber matrix adhesion.

## EXPERIMENTAL

### Materials

The materials employed in this investigation were propylene–ethylene random copolymer (PPE) matrix (density, $\rho = 0.905$ g cm$^{-3}$, MFI = 0.8 dg/min, melting temperature = 147.5°C, ~ 5% ethylene), PP with 10% titanium dioxide (to enable measurement of matrix concentration), and PP fibers (diameters = 50 $\mu$m). Some of the physical properties of these fibers are listed in Table I. Note that the densities differ from that of pure PP due to the presence of filler, that is, delusterant or pigment, in the fibers. The PP fibers were washed with commercial acetone to remove any processing lubricants. Fiber diameters were measured by using optical microscopy after calibration with a standard grid glass slide. The fibers were treated under the same condition as was used for composite preparation to show the effect of these conditions on the fiber stiffness but in this case the fibers were clamped between two clamps (to allow for similar

**TABLE I**
**Properties of Polypropylene Fiber**

| Sample | Fibre diameter ($\mu$m) | Tensile strength (MPa) | Tensile modulus (GPa) | | Length (cm) | Density ($gcm^{-3}$) |
|---|---|---|---|---|---|---|
| | | | Before treatment | After treatment | | |
| Polypropylene fiber | 50 | 250–350 | 5.1 ± 0.3 | 4.7 ± 0.4 | 2.3 ± 0.5 | 0.91 |

thermal relaxations). The tensile properties are listed in Table I.[15] The fibers were obtained from Melded Fabrics Pty. Ltd. (Melbourne, Victoria, Australia); the PPE was obtained from Basell Australia Pty. Ltd. (Geelong, Victoria, Australia), and PP with titanium dioxide was obtained from Ciba Pty. Ltd. (Thomastown, Victoria, Australia).

### Composite preparation

PPE and PP with titanium dioxide with a composition of 5–7% PP with titanium dioxide and 93–95% PPE were compounded in a Brabender twin-screw extruder to prepare a blend film for the composites. A barrel temperature of 150°C and die temperature of 160°C were used. Blend compositions were mixed manually and thoroughly prior to being fed into the extruder hopper.

For PP–PPE composites, the processing temperature is important to maximize the fiber–matrix adhesion and to keep the original fiber morphology because the reinforcement and the matrix are of similar materials. Choosing the conditions for the composite preparation was based mainly on the information obtained from differential scanning calorimetry (DSC) experiments,[14] considering that the processing temperature should be higher than the melting temperature of the PPE (147°C, measured by DSC) and lower than the melting temperature of the fibers (164°C). At higher temperatures, the degree of orientation will decrease and the fiber properties would deteriorate. Between 152 and 157°C, because of a lower degree of orientation in the fiber skin, most of the relaxation is expected to occur there, rather than in the fiber core, resulting in relaxing or partial melting, which in turn, produces favorable conditions for bonding at the fiber–matrix interface. The heated press method used for composite preparation consisted of two stages. In the first stage, long PP fibers were distributed randomly on top of the film of the blend of PPE and PP with titanium dioxide film (~ 0.2–0.4 mm thickness) and placed between two Teflon sheets and then pressed at 152–157°C for 5–7 min. After that, an 11- to 14-kPa pressure was applied for 8–10 min. In the second stage, three layers of the composite prepared according to the previous stage were laminated together in different directions to provide a composite with more random fiber distribution and uniform composition. The laminated fiber composite has potential application as paneling, whereas a single composite layer provided a useful reinforced PP. The fiber volume content of the PP–PPE composites varied between 10 and 60%.

### Differential scanning calorimetry

A DSC (Perkin–Elmer Pyris 1) was used for thermal analysis of the pure polymer, fibers, and composites. Samples of ~ 3 mg were placed and sealed in 10-$\mu$L aluminum pans. A constant nitrogen flow of 40 mL/min was used to purge the instrument. The samples were held at 30°C for 2 min, then heated from 30 to 180°C at a rate of 10°C/min, held at 180°C for 2 min, cooled to 30°C at the same rate, and held for 2 min. A second heating scan to 180°C was then performed. The first heating scan melted both the matrix and the fibers. $T_c$ was measured from the peak of the exotherm during cooling. The second heating cycle provided results that were more consistent for the melting temperatures ($T_m$) measured from the peak of the endotherms. The instrument was calibrated for temperature by using indium and lead and calibrated for enthalpy by using indium, and a furnace calibration was performed according to the manufacturer's recommendations. A conditioning scan was performed before any data collection scans. A baseline with matched empty pans was used to convert the data to apparent specific heat to allow direct comparison of all curves. In the specific heat convention, both the endotherm on heating and the exotherm on cooling are shown as positive. For clarity of presentation, successive curves have been shifted by 5 units in Figure 1.

### Static mechanical analyses

The mechanical properties were determined from six samples of each composite with a Perkin–Elmer DMA 7e in extension and three-point bend modes. The static force ranged from 100 to 8000 mN at 100 mN/min and 0.0 to 6400 mN at 400 mN/min for three-point bend and extension modes, respectively. The maximum displacement can be measured with this instrument at about ±5 mm. The composite samples were cut along a range of orientation on the sheets, to provide dimensions of 1 × 12 × 5 and 1 × 10 × 5 mm for three-point bend and extension modes, respectively. The sample dimensions were kept as similar as possible to obtain

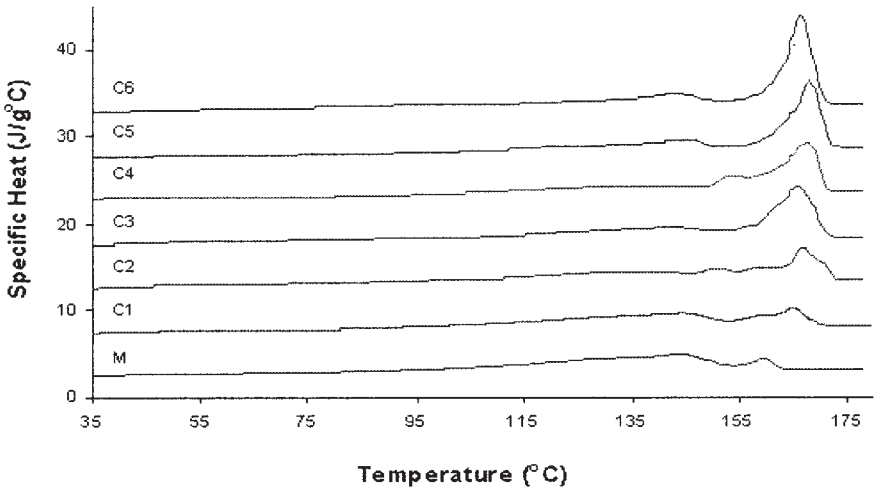


(a)

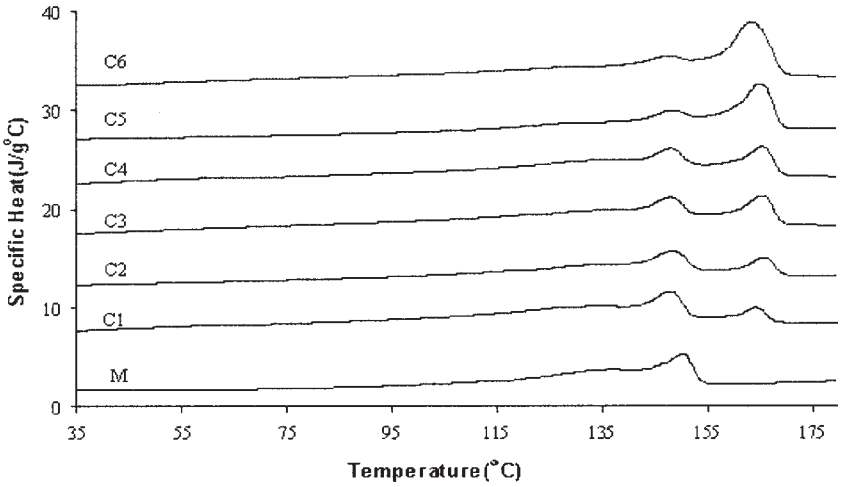


(b)

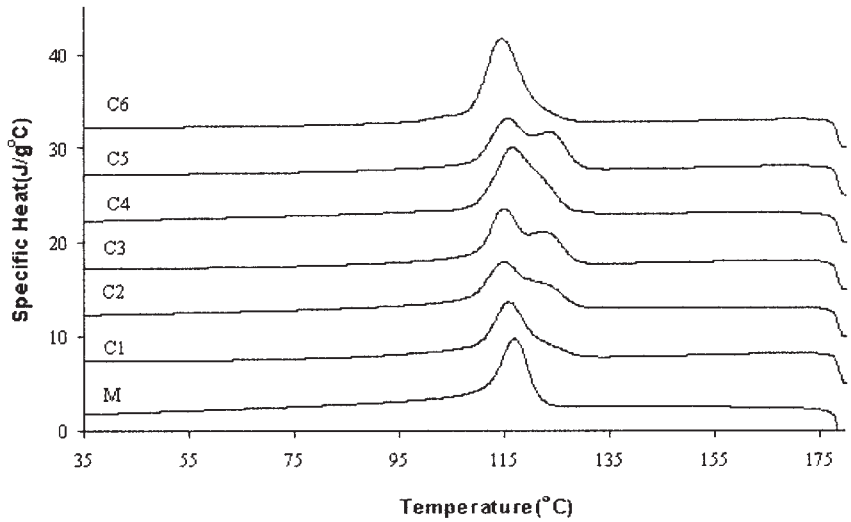


(c)

**Figure 1** DSC melting (first heating) (a), second heating (b), and crystallization (cooling after first heating) (c) of polypropylene fiber–matrix composites.

**TABLE II**
**Thermal Properties of Polypropylene Fiber–Matrix Composites ($T_c$'s, $X_c$, $T_m$'s, $X_m$)**

| Sample | Designation | Fiber fraction (wt%) | $T_C$ (°C) | $X_C$ (%) | $T_{M1}$ (°C) | $T_{M2}$ (°C) | $X_M$ (%) |
|---|---|---|---|---|---|---|---|
| PPE | $M$ | — | 116 | 36 | 147 | — | 38 |
| | $C_1$ | 10 | 115 | 32 | 148 | 164 | 25 |
| | $C_2$ | 20 | 114 | 34 | 148 | 165 | 34 |
| Composite | $C_3$ | 30 | 114 | 35 | 149 | 166 | 38 |
| | $C_4$ | 40 | 116 | 40 | 149 | 166 | 41 |
| | $C_5$ | 50 | 115 | 43 | 148 | 166 | 52 |
| | $C_6$ | 60 | 114 | 45 | 148 | 163 | 54 |

a reliable comparison between the mechanical properties from different composites. The instrument was calibrated for force by using a standard mass and distance by using a standard steel block.

### Dynamic mechanical analysis

Dynamic mechanical analysis (DMA) was performed in three-point bend mode by using a Perkin–Elmer DMA 7e with an Intercooler II. A dynamic force of 450 mN and static force of 600 mN were used with a frequency of 10 Hz and the temperature scan ranged from –50 to 100°C at 2°C/min. A constant nitrogen flow of 40 mL/min was used to purge the instrument. The frequency scans ranged from 1 to 30 Hz at 1 Hz/min at temperatures of −50, −25, 0, 25, 50, 75, and 90°C. The composite samples were cut along a range of orientations on the sheets, with dimensions 1 × 10 × 5 mm. The sample dimensions were kept as similar as possible to obtain a reliable comparison between the results from different composites. Storage and loss moduli were recorded as a function of temperature and frequency, and loss modulus was plotted as a function of storage modulus in the Cole–Cole analysis. The instrument was calibrated for temperature by using indium force using a standard mass; probe position, furnace, and eigenvalue calibrations were also performed.

### Thermogravimetry (TGA)

The compositions of the specimens were analyzed by using four samples for each composite including 10% PP with titanium dioxide with a Perkin–Elmer TGA 7. Specimens, weighing 8–15 mg, were heated from 30 to 600°C at 20°C/min under a nitrogen purge and then heated to 800°C at the same rate but under an air purge. The instrument temperature calibration was performed by using the Curie temperature of various metals according to the manufacturer's recommendations.

## RESULTS AND DISCUSSION

### DSC measurements

The effect of the fibers on the thermal properties of PP was analyzed by DSC. Thermal parameters such as $T_m$, crystallization temperature ($T_c$), and the crystallinity ($X_c$) of the composites were measured and the results are presented in Table II. Figure 1(a, b, c) shows the DSC thermograms of the matrix and composites. As seen in Figure 1, the fibers melt at a higher temperature than does the matrix, which facilitated molding of the composites. Because the molding temperature is between the melting temperatures of fibers and matrix, melted matrix filled the spaces between the fibers during the compression-molding process.

In the case of PP composites, the endothermic peak at higher temperature was due to the fibers, so relative crystallinity was determined and used to calculate the fiber volume fraction. The lower temperature endotherm corresponds to the melting of spherulites in the bulk of the random PPE matrix. Also, a shoulder appears in front of the melting peak in the first heating curves, which may be due to the transcrystalline phase, recrystallization, or reorganization of crystals initially formed during the preparation. Microscopic analysis of the PP–PPE composites in polarized light also revealed a transcrystallinity of the matrix around the fibers as shown in Figure 2, as previously discussed.[15] This new morphology of the matrix seems to modify slightly the temperature where melting occurs. However, the melting peaks are not influenced appreciably by the fiber (e.g., the transcrystallization or recrystallization effects).[7] Moreover, Figure 1(b) shows typical DSC curves corresponding to the second heating scan of PP composites containing 10, 20,

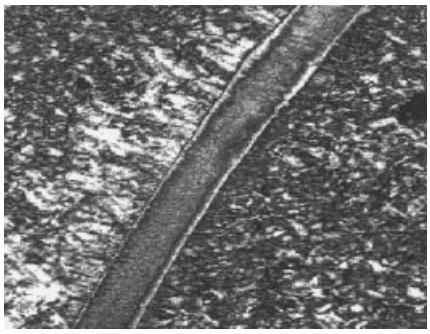

**Figure 2** Optical microscopy showing morphology about a single fiber (magnification, ×400).

**TABLE III**
**Expected and Experimental Values for the Fiber Fraction in the Composites**

| Sample | Designation | Theoretical fiber fraction (wt %) | Experimental fiber fraction (wt %) | The ratio between polymer and titanium dioxide (%) | Void (%) |
|---|---|---|---|---|---|
| Matrix | $M$ | 0 | 0 | 24.6 | |
| | $C_1$ | 10 | 12 ± 1 | 12.6 | 0.1 |
| | $C_2$ | 20 | 24 ± 1 | 23.8 | 0.5 |
| Composite | $C_3$ | 30 | 29 ± 1 | 29.5 | 0.5 |
| | $C_4$ | 40 | 40 ± 1 | 40.1 | 3.9 |
| | $C_5$ | 50 | 50 ± 1 | 50.9 | 4.6 |
| | $C_6$ | 60 | 56 ± 3 | 60.2 | 19.3 |

30, 40, 50, and 60 wt % fiber, respectively. It is clear from Table II and Figure 1(b) that the addition of PP fibers to PPE caused only a marginal effect on $T_m$ and no correlation of the results with the fiber concentration can be established. Furthermore, a shoulder appeared on the exothermic peak, which is due to the fiber crystallization, followed by the peak related to the matrix transcrystallization and crystallization.

A key characteristic of the PPE is the degree of crystallinity, which especially controls its mechanical properties. The crystallinity of these PP composites were determined by using the relationship $X_c = \Delta H_f^\circ / \Delta H_f^\circ w$,[7] where a value of $\Delta H_f^\circ = 209$ J/g was taken for 100% crystalline PP and $w$ is the mass fraction of PP in the composite.

It is clear from Figure 1(c) and Table II that the addition of PP fiber to PPE results in an increase in $X_c$ and $T_c$ of the PPE matrix. This can be explained as being due to the nucleating ability of the PP fiber for the crystallization of PPE matrix. It can be attributed to the fact that, although the original fiber and crystalline structure were melting, preferred molecular orientation was still present, facilitating transcrystallinity in the matrix. As the amount of the added fiber increased, $T_c$ also was found to increase. $T_c$ and enthalpy of crystallization ($\Delta H_f^\circ$) of the PP phase increased with increasing content of PP fibers, indicating that PP fibers nucleate the crystallization process.

## Fiber concentration

Thermogravimetric results of PP–PPE composites are reported in Table III and show excellent agreement between experimental and calculated fiber content. For measurement of the amount of fibers in the composite, for instance, composite $C_3$, the amount of added titanium dioxide was measured in the unfilled polymer. The ratio between polymer and titanium dioxide in the unfilled polymer was 24.6%. Table III shows the ratio between polymer and titanium dioxide in different composites. In view of the amount of titanium dioxide in the composite, the amount of matrix polymer was measured. It is known that

$$V_f + V_m + V_t = 1 \quad (7)$$

where $V$ is a volume fraction and subscripts $f$, $m$, and $t$ represent fiber, polymer, and titanium dioxide, respectively. Then, the fiber fraction in the composite was calculated as 28.5%, in composite $C_3$. The fiber concentration in all composites was measured in the same way.

## Mechanical properties

### Static mechanical properties

The results for the tensile and flexural modulus as functions of fiber concentration are shown in Figure 3(a, b). The tensile and flexural properties of the composites were strongly influenced by fiber fraction. The tests showed a strong influence of crystallinity on the mechanical performance of the matrix. The slope of the stress–strain curves at a low elongation (<1%), indicating the elastic modulus of the composites, mainly depends on both the matrix and the fiber characteristics as well as on the interaction of the fiber–matrix interface. In both data sets, flexural and tensile modulus, it can be assumed that the composite stiffness clearly shows a dramatic increase with increasing fiber concentration. This is due to the fact that the reinforcement imparted by the fibers allows stress transfer from the matrix to the fibers. At low fiber concentration, the matrix is not restrained by enough fibers and highly localized strains occur in the matrix at low stresses. As the fiber concentration increased up to 50%, the stress was more evenly distributed and the composite stiffness increased. The composite containing 60% of fibers was somewhat lower than the trend, particularly in the bending test. The deviation at very high fiber concentration may be due to the (1) fiber packing and (2) insufficiently rich polymer regions. The possibility of fiber entanglements, in the composite with random fibers, increases as the fiber concentration increased. Although this results in a higher stiffness in the out-of-plane direction and a subsequent decrease in stiffness in-plane, this effect is more

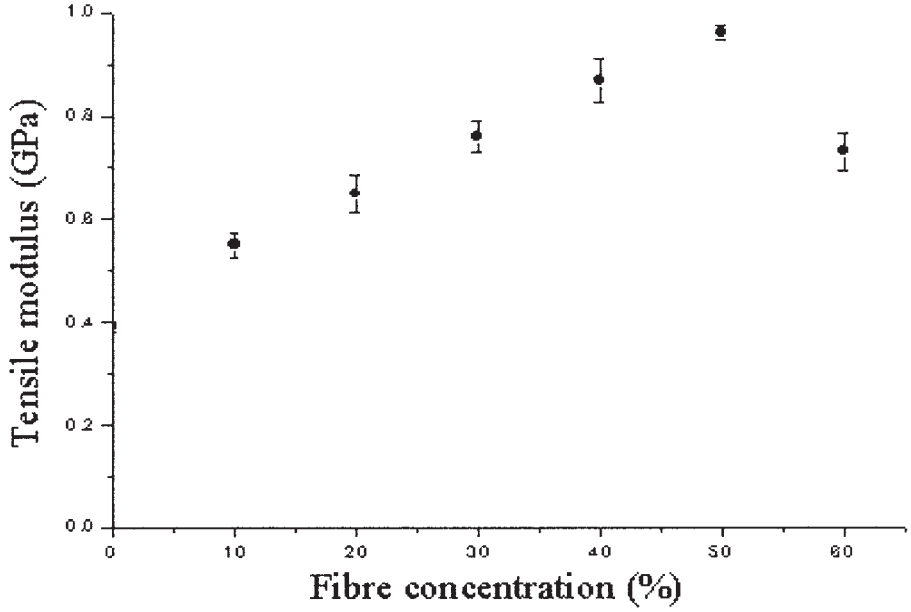


(a)

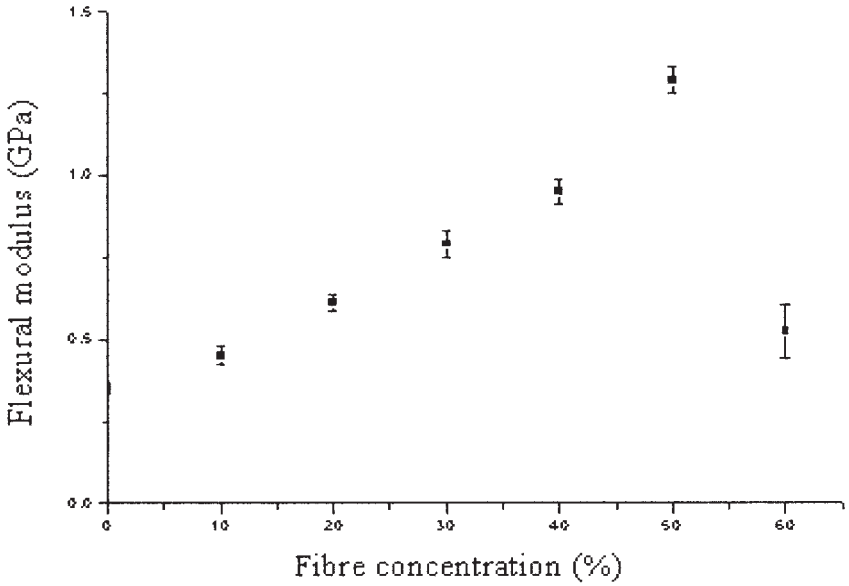


(b)

**Figure 3** Tensile (a) and flexural (b) modulus for the polypropylene fiber–matrix composites with different fiber loadings.

pronounced in compression testing than tensile testing.[1,18] Thus, the greater sensitivity of the bending data can be explained as due to both the compressive and the extension forces during the test. Another reason for this deviation is that insufficient matrix was available and indicates that there are areas of insuffi-

**TABLE IV**
**Experimental and Theoretical Tensile Modulus for Different Fiber Concentrations**

| Sample | Fiber fraction (wt %) | Designation | Tensile modulus 25°C (GPa) | | |
|---|---|---|---|---|---|
| | | | Exp. | Cox equation | Halpin–Tsai equation |
| Composites | 10 | $C_1$ | 0.55 ± 0.03 | 0.58 | 0.41 |
| | 20 | $C_2$ | 0.65 ± 0.04 | 0.70 | 0.44 |
| | 30 | $C_3$ | 0.76 ± 0.03 | 0.78 | 0.51 |
| | 40 | $C_4$ | 0.87 ± 0.04 | 0.93 | 0.58 |
| | 50 | $C_5$ | 0.96 ± 0.02 | 1.02 | 0.67 |
| | 60 | $C_6$ | 0.73 ± 0.51 | 0.80 | 0.59 |

cient matrix between the fibers. This means the fibers were no longer completely surrounded by the matrix at very high fiber concentration and voids are produced in the composite. It has been reported[21] that most of the properties of composites are affected by the presence of voids. For instance, the interlaminar shear strength of brittle composites decrease by about 7% for each 1% of voids present.[21] The void content and distribution depend on some important factors, such as fiber concentration, distribution, and matrix properties. This can result from incomplete wetting of the fibers by the matrix; thus, it can be assumed that the deviation at high fiber concentration is because of the increase of void content. To check this hypothesis, we calculated the density of the composites from their weight and dimensions, using the density of the fiber and matrix, which are shown in Table I, and the results, which are shown in Table III.

$$V_v = [1 - (d_c/W_c)((W_f/D_f) + ((W_c - W_f)/D_m))] \quad (8)$$

where $V$ is void volume fraction, $W$ is weight, $d$ is density, and subscripts $f$, $m$, and $c$ represent fiber, polymer, and composite, respectively.[1,21]

This indicates that the void content of the samples with 10–30% w/w are ~ 0. However, the 60% w/w sample has a void content of 19.3%, which is a confirmation for the hypothesis that there is incomplete wetting of the fibers by the matrix, leading to entrapment of air. This is most likely to occur in systems where the dry fibers were closely spaced and the viscosity of the matrix is high.

Calculation of modulus used eq. (6), with the input parameters and results, are shown in Tables I and IV, respectively. It can be seen that the theoretical tensile modulus showed good agreement with experimental values up to 60% fiber, but the stiffness of this composite was overestimated and the experimental data fell below the theoretical data. As previously discussed, this deviation can be explained as due to the fiber packing problem, out-of-plane or bent fiber, and void content. We assumed that, when the number of fibers exceeded 50%, there was insufficient matrix available to fill the gap between the fibers and this can be a reason for producing voids, which reduce the stiffness of the composite. As mentioned above, the void content is ~ 20% for this composite, which is 20 times more than the void content in other composites. If this actual fiber concentration and tensile modulus were used in eq. (6), a value of 0.8 GPa was obtained, which is very close to the experimental value. Another equation was introduced by Halpin–Tsai.[22] Composite theory is put in the form

$$E_f = E_m(1 - ABV_f)/(1 - BV_f) \quad (9)$$

where

$$B = (E_f/E_m - 1)/(E_f/E_m + A) \quad (10)$$

where $A = 2(l/d)$ for tensile modulus. The ratio $l/d$ is the aspect ratio. This self-consistent method, which has served as the function for eq. (9), was applied more rigorously to short fiber composites.[22] The results from this equation are shown in Table IV. However, there is a high deviation from the experimental values due to the nature of the Halpin–Tsai theory, which is mostly used for short fiber composites.

## Dynamic mechanical properties

To analyze the effect of the fiber concentration on the dynamic properties of the composites, the dynamic mechanical properties were measured. The storage modulus as a function of temperature at a frequency of 10 Hz is shown in Figure 4(a). The results show the effect of fiber concentration on the stiffness of the laminates. Fibers have a large effect in improving the modulus of materials. It can be seen that the addition of fibers increased the modulus sharply; at any particular temperature, the $E'$ increased with fiber concentration, because of the combination of the effect of the fibers embedded in a viscoelastic matrix and to the mechanical limitation introduced by the fibers at high concentration, which reduce the mobility and deformation of the matrix. Other authors have also reported

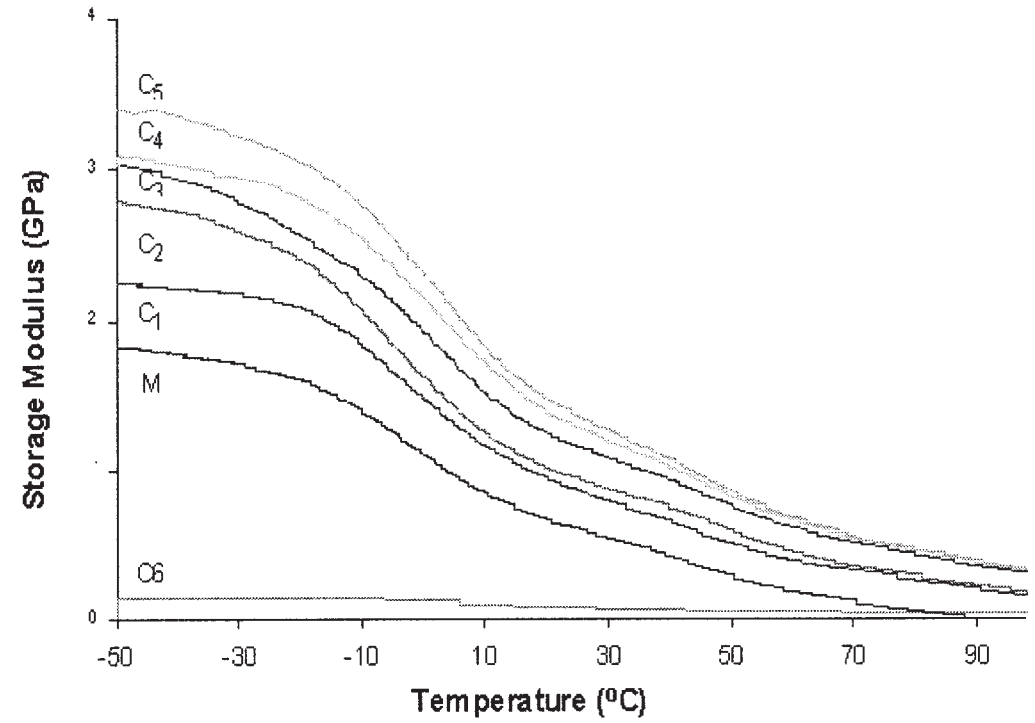


(a)

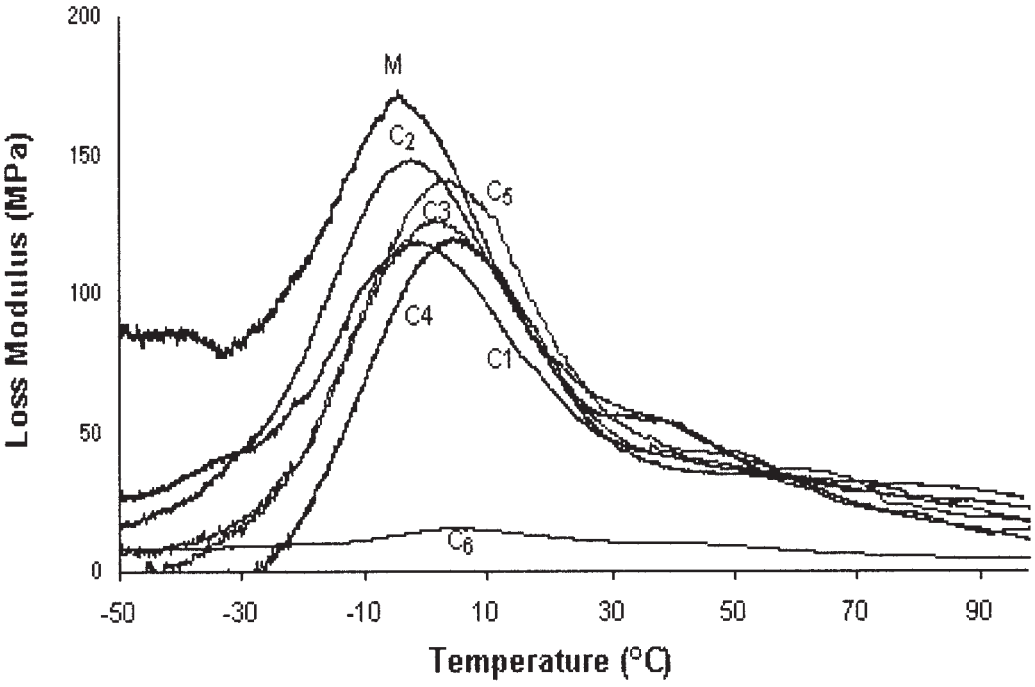


(b)

**Figure 4** Dynamic mechanical analysis of polypropylene fiber–matrix composites using three-point bend configuration: (a) storage modulus, (b) loss modulus.

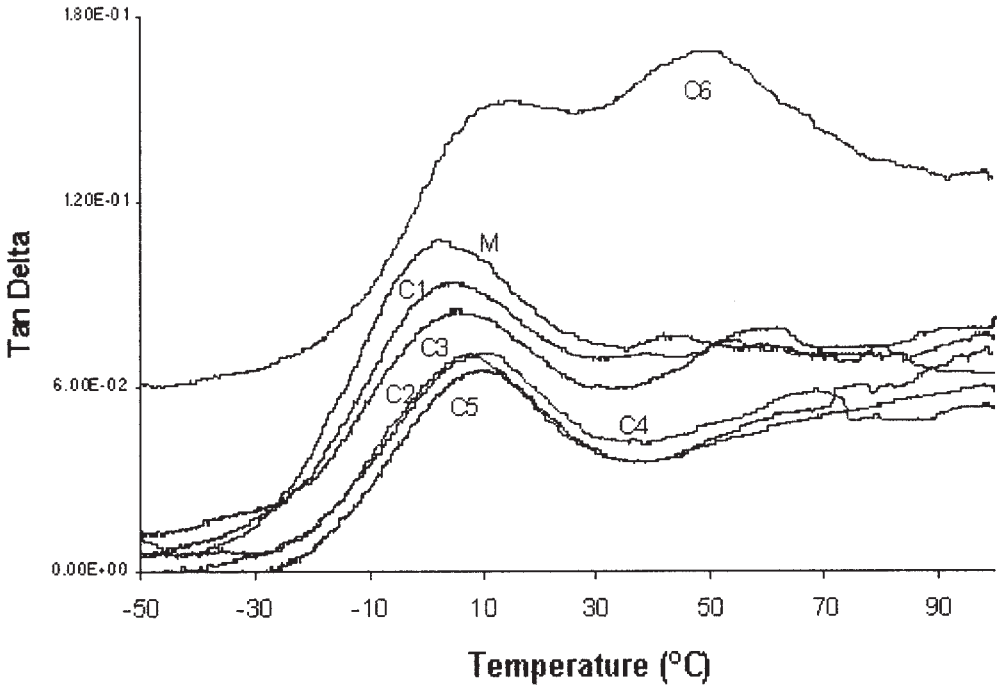


(c)

**Figure 4** (*Continued from the previous page*)

similar observations.[23,24] At temperatures below $T_g$, the storage modulus of the matrix and composite are very close to each other, because of the less contribution of fiber to imparting the stiffness to the other materials at low temperature. As expected, the modulus decreased when the temperature increased, due to softening of the matrix and initiation of relaxation processes and melting. Modulus decreases, whereas molecular mobility and thermal expansion increase on going through $T_g$, and a peak in loss modulus and tan $\delta$ occurred and caused an increase in the separation of fibers, which reduced intermolecular forces. This re-

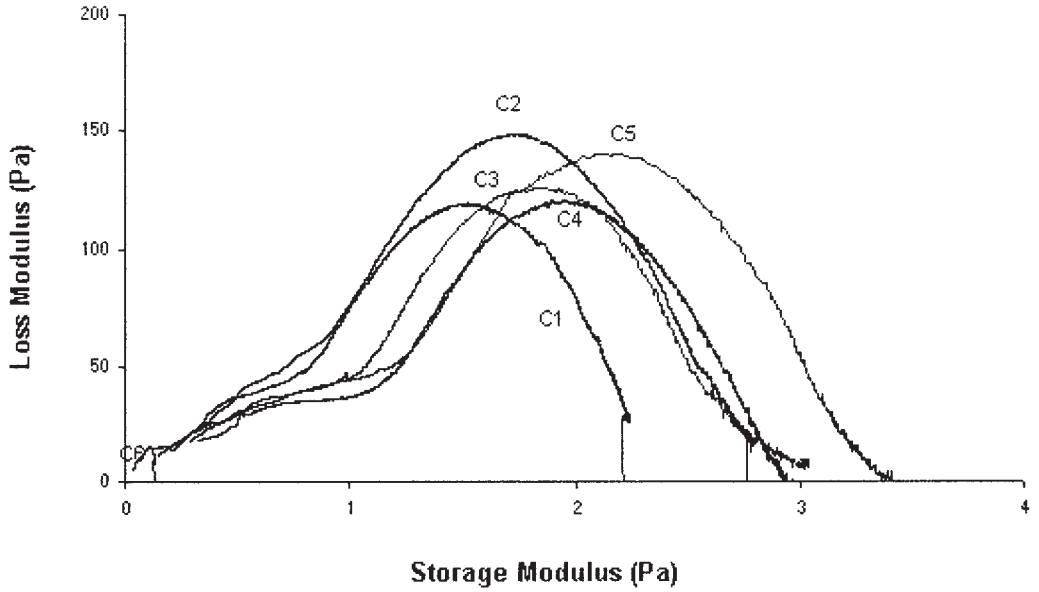


**Figure 5** Cole–Cole plots of composites with different fiber concentrations.

**TABLE V**
**The Value of the Constant *C***

| Sample | Fiber fraction (%) | *C* |
|---|---|---|
| Composite | 10 | 1.00 |
| | 20 | 1.00 |
| | 30 | 0.98 |
| | 40 | 0.91 |
| | 50 | 0.87 |
| | 60 | 0.97 |

duction in the modulus is very high for unfilled systems because of the stiffness at high temperature being determined by the amorphous regions. However, in the case of composites with higher fiber concentration, the decrease in stiffness with temperature was less pronounced. The effectiveness of the fibers on the modulus of the composite can be represented by a coefficient factor $C$[23]

$$C = (E'_g/E'_r)_c/(E'_g/E'_r)_m \quad (11)$$

where $E'_g$ and $E'_r$ are the storage modulus in the glassy and rubbery region and the subscripts $c$ and $m$ represent composite and matrix, respectively.

The lower the value of this constant, the higher effectiveness of the reinforcement. Measured storage modulus at −30 and 0°C at a frequency of 10 Hz were employed as $E'_g$ and $E'_r$, respectively, and the results are listed in Table V. In this case, the lowest value was obtained for the composite with 50% fiber concentration and the highest value was obtained for the composite with 10% fiber concentration. Figure 4(a) shows the storage modulus at different temperatures as a function of fiber concentration. As it can be seen from this figure, the value of storage modulus of all composites increases up to 50% fiber concentration in the composite and then decreases.

Figure 4(b) shows the loss modulus as a function of temperature for the systems with different fiber concentrations at a frequency of 10 Hz. The loss modulus is indicative of the material's ability to dissipate mechanical energy, which is proportional to sample damping (viscous behavior) and impact resistance of the material. It provides much information on the overall flexibility and interactions between the components of composite materials.[18,23,26] Compared with the PPE matrix, $E''$ of the composites became broadened and extended to the higher temperature side with an increase in fiber concentration up to 50%. Table VI shows the values of peak height and width of tan δ with fiber concentration, and there is a regular decrease with increasing fiber concentration in the peak height. This means that as the fiber concentration increases up to 50%, the most predominant effect of the reinforcement has been the flattening and broadening of the transition region, which would make the $E''$ peak broader. As reported before, it can be explained because of the difference in the physical state of the matrix surrounding the fibers to the rest of the matrix and immobilized polymer layer matrix.[6,23,25] However, there is an anomaly for 60% fiber concentration due to the fiber packing problems and void content, as previously discussed.

Figure 4(c) shows the tan δ as a function of temperature. As shown in Figure 4(c), the relaxation peak is located at ~ 4.0°C (β-relaxation). The dominant β-relaxation corresponds to the glass–rubber transition of the amorphous portions and the temperature of the peak maximum is assigned to the $T_g$ of the matrix. Also maximum heat dissipation occurs at this temperature. After the glass transition range, a slight rubbery plateau can be observed between $T_g$ and $T_m$. As Chua reported, a composite with poor interfacial bonding tends to show more energy than that with good interface bonding.[25] It can be associated with a reduction in the mobility of the chains by the addition of PP fibers into the matrix. This means that, the higher the damping at the interface, the poorer the interfacial adhesion. When the fiber concentrations are very low, fibers will be too far apart for effective stress transfer from matrix to fiber in the composite, which leads to easier failure of the interfacial bonding. By increasing the fiber concentration, there is closer packing of the fibers, which causes efficient stress transfer, whereas by increasing fiber concentration > 50%, and there is not sufficient polymer to wet and pack the fibers completely, which leads to fiber-rich region. Thereby fibers cannot contribute to imparting stiffness to the materials. On increasing the fiber concentration in the composites, the position of the β-relaxation or $T_g$ was shifted to the higher temperature, which shows the effectiveness of fiber–matrix interaction. It can be associated with the decrease in mobility of the polymer by addition of fiber. Furthermore, the width of this peak is shown in Table VI. The width of the tan δ became wider by increasing fiber concentration, suggesting the molecular relaxation and motion at the interfacial region, which contribute to the damping of the material apart from the reinforcement and matrix.[6,23,25] The observed

**TABLE VI**
**Peak Height and Width of the tanδ**

| Sample | Fibre fraction (%) | Peak height (MPa) | Peak width (MPa) |
|---|---|---|---|
| PPE | — | 3.2 | 3.3 |
| Composite | 10 | 2.9 | 3.2 |
| | 20 | 2.2 | 4.1 |
| | 30 | 2.8 | 3.9 |
| | 40 | 2.4 | 4.2 |
| | 50 | 2.2 | 4.0 |
| | 60 | 3.0 | 6.4 |

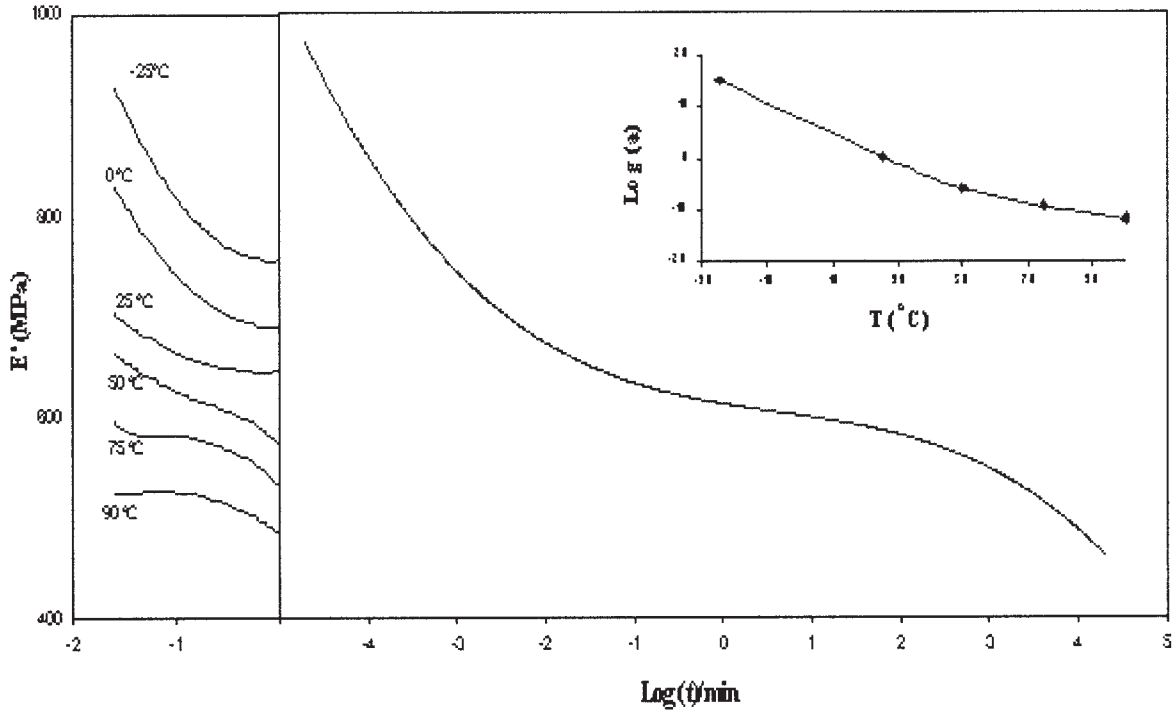


**Figure 6** Modulus–time master curve based on time–temperature superposition (TTS) of data for 50%.

reduction in the intensities of the $\beta$-transition peak for the composite may be attributed to the formation of an immobilized shell of polymer around each fiber, which restricted small main-chain motions within the shell. The occurrence of this polymer shell with modified properties may be induced by morphological changes such as transcrystallinity and crystallization of crystallizable matrix, and adsorption of the matrix onto the surface of the fiber in the polymer. The result is that the energy dissipation and molecular damping can be affected by adhesion.

## Cole–Cole analysis

Figure 5 shows a Cole–Cole plot, where the loss modulus ($E''$) is plotted as a function of the storage modulus ($E'$). It was reported that two-phase systems are typically depicted as two modified circles, whereas homogeneous polymeric systems show a semicircle. In the present case, the curve represents an imperfect semicircle; it can be assumed that the composite's behavior is slightly different from homogeneous polymeric system behavior and this may be due to the presence of the fibers, different phases, and interphase behavior. Although the matrix and fibers are of the same polymer, the composite is not indicative of a homogenous system.

## Time–temperature superposition (TTS)

The viscoelastic properties of materials are dependent on temperature and frequency (time). A dynamic measurement is conducted over a frequency range at constant temperature or over a temperature range at constant frequency. If a material is subjected to constant stress, its elastic modulus will decrease over a period of time due to molecular rearrangement acting to minimize the localized stress. Modulus measurements performed over a short time (high frequency) result in a high modulus, whereas measurements taken over a long times (low frequency) result in a lower modulus.[27]

The storage modulus of the PP–PPE composite as a function of time is shown in Figure 6. At a given temperature, the value of $E'$ tends to increase due to the lower mobility of polymeric chains at higher frequency. The viscoelastic properties at a given frequency are quantitatively equivalent to those of an experiment carried out over a time $t = 1/2\pi f$. The modulus curve at a particular temperature is then shifted along the time axis until it overlaps with the next curve. The temperature of 25°C was taken as the reference temperature and the distance between curves gives the shift factor $a_T$ by an amount[26,27]

$$\text{Log } (a_T) = \text{Log } \omega_s - \text{Log } \omega = \text{Log } (\omega_s/\omega) \quad (12)$$

or

$$\text{Log } a_T = (-C_1(T - T_s))/(C_2 + (T - T_s)) \quad (13)$$

where $C_1$ and $C_2$ are constants, $\omega$ is frequency, $T$ is temperature, and subscript $s$ is the reference curve.

This factor characterizes the rate of relaxation mechanism at the same temperature $T_i$ in composites with the rate at a higher temperature $T_{i+1}$. In this way, $\log(a_T)$ values for each temperature were determined. Figure 6 shows the $E'$ versus $\log f$ graph for temperatures from $-25$ to 100°C. These experimental curves of the modulus for different temperatures are plotted against $\log f$. By using the time–temperature–superposition principle, it can be seen that there is a dramatic decrease in the elastic modulus of the composite; also the elastic modulus and composite stiffness can be extrapolated over a long term.

## CONCLUSION

The preparation of novel composite materials consisting of PP fibers and a PPE matrix was described. They are strongly bonded to each other without any surface treatment. In this study, the effect of the fiber concentration on the structural, thermal, and mechanical properties of PPE was analyzed by static and DMA and DSC.

The study performed by DSC revealed an increase of the melting temperature with the introduction of PP fibers. The results demonstrate no significant shift in the crystallization temperature or the final melting temperature by changing the fiber concentration in the composite.

The incorporation and increase of the fiber concentration gave rise to a considerable increase of the tensile, flexural, and storage modulus. The maximum improvement in properties was observed for the composite with 50% fiber concentration, which is chosen as the critical fiber concentration. This was due to the reinforcement imparted by the fibers that allowed stress transfer from the matrix to the fibers. However, there was a deviation at high-fiber volume fraction more than a critical value, which was due to the lack of matrix and fiber packing problems and a consequential increase in void content. The positions of the relaxations in amorphous region were affected by the addition of fiber and show the adhesion between two phases. The loss modulus peak became broader and flatter, which emphasized the improved fiber–matrix adhesion. A Cole–Cole curve depicts the heterogeneity of the systems as well as the good interfacial adhesion at high fiber concentration except at greater than critical fiber concentration. The TTS plot is useful in predicting the long-term behavior of the PP–PPE composite.

Financial support from International Postgraduate Scholarship (IPRS) is acknowledged.

## References

1. Thomason, J.; Vlug, M. A. L. Compos A: Appl Sci Manufact 1996, 27, 477.
2. Saujanya, C.; Radhakrishnan, S. Polymer 2001, 42, 4537.
3. Schwartz, M. Composite Materials Handbook; McGraw-Hill: New York, 1984; pp 1.1–2.5.
4. Stern, T.; Teishev, A.; Marom, G. Compos Sci Technol 1997, 57, 1009.
5. Thomason, J. L.; Van Rooyen, A. A. J Mater Sci 1992, 27, 889.
6. Amash, A.; Zugnmaier, P. J Appl Polym Sci 1997, 63, 1143.
7. Joseph, P. V.; Joseph, K.; Thomas, S.; Pillai, C. K. S.; Prasad, V. S.; Groeninckx, G. Composite A 2003, 34, 253.
8. Devaux, E.; Caze, C. Compos Sci Technol 1999, 59, 459.
9. Karger-Kocsis, J. Polypropylene: Structure Blends Composites, Vol. 1; Chapman and Hall: London, 1995; pp 1–50.
10. Karger-Kocsis, J. Polypropylene: Structure Blends Composites, Vol. 3; Chapman and Hall: London, 1995; pp 71–202.
11. Mallick, P. K.; Newman, S. Composite Materials Technology; Hanser: Munich, Germany, 1990.
12. Loos, J.; Schimanski, T.; Hofman, J.; Peijs, T.; Lemstra, P. J. Polymer 2001, 42, 3827.
13. Poldervaart, T. Eur. Pat. Appl. EP 888883, 6, 1999.
14. Houshyar, S.; Shanks, R. A. Macromol Mater Eng 2003, 288, 599.
15. Houshyar, S.; Shanks, R. A. Polym Int to appear.
16. Hine, P.; Ward, I.; Jordan, N.; Olley, R.; Bassett, D. C. Polymer 2003, 44, 1117.
17. Jordan, N.; Bassett, D.; Olley, R.; Hine, P.; Ward, I. M. Polymer 2003, 44, 1133.
18. Robinson, I. M.; Robinson. J. M. J Mater Sci 1994, 29, 4663.
19. Cox, H. L. J Appl Phys 1951, 3, 72.
20. Rosethal, J. Polym Compos 1992, 13, 462.
21. Farouk, A.; Langrana, N. A.; Weng. G. J. Polym Compos 1992, 13, 285.
22. Chow, T. S. J Mater Sci 1980, 15, 1873.
23. Pothan, L. A.; Oommen, Z.; Thomas, S. Compos Sci Technol 2003, 63, 283.
24. Menard, K. P. Dynamic Mechanical Analysis; CRC Press: Boca Raton, FL, 1997; pp 50–70.
25. Joseph, P. V.; Mathew, G.; Joseph, K.; Greninckx, G.; Thomas, S. Composites A 2002, 34, 275.
26. Ibarra, L.; Macias, M.; Palma, E. J Appl Polym Sci 1995, 57, 831.
27. Cardon, A. H.; Verchery, G. Durability of Polymer Based Composite Systems for Structural Applications; Elsevier: London, 1990; p 428.